PROCEEDINGS OF SCIENCE

Transverse momentum correlations in p-Pb and Pb-Pb collisions in ALICE at the LHC

Prabhat Pujahari (for the ALICE collaboration)
Department of Physics and Astronomy, Wayne State University, Detroit, USA
E-mail: p.pujahari@cern.ch

Abstract. Two-particle correlations provide information about particle production mechanisms in heavy-ion collisions. We report on the study of two particle transverse momentum correlations ($\Delta p_{\rm T}\Delta p_{\rm T}$) in Pb-Pb collisions at $\sqrt{s_{\rm NN}}$ = 2.76 TeV and in p-Pb collisions at $\sqrt{s_{\rm NN}}$ = 5.02 TeV measured with the ALICE detector. Unlike the particle number correlation functions, $\Delta p_{\rm T}\Delta p_{\rm T}$ measures transverse momentum correlations between particle pairs. The $p_{\rm T}$ dependence of this correlation measure may make it amenable to probe the fluctuations in temperature, average momentum, flow, hardness of spectrum and hardness of correlations (jet vs non-jets). Correlation functions for ++, −−, +−, and −+ charged particle pairs as a function of pair azimuthal and pseudo-rapidity separation ($\Delta\varphi$, $\Delta\eta$) are measured. The information from the above charged pairs are combined into a charge independent (CI) correlation. We study their evolution with collision centrality and particle multiplicity per event. We find that $\Delta p_{\rm T}\Delta p_{\rm T}$ correlation shapes exhibit a strong centrality dependence in Pb-Pb collisions and multiplicity dependence in p-Pb collisions. The correlation function is everywhere positive, indicating that both particles from a pair are more likely to have momentum above or below the average transverse momentum in an event ensemble. We further study the Fourier decomposition of the correlation functions dependence on $\Delta\varphi$ as a function of $\Delta\eta$.

1. Introduction

Two-particle correlation functions measured at RHIC and the LHC energies have shown unanticipated structures both on the near- and away-side [1, 2, 3, 4]. There remains ambiguity, however. In an effort to lift some of these ambiguities, it is interesting to consider additional observables and types of correlation functions. In this work, we present measurements of R_2, a number correlation function, which we complement with measurements of a transverse momentum correlation function, $\Delta p_{\rm T}\Delta p_{\rm T}$ [5]. These two correlation functions are studied in p-Pb collisions at $\sqrt{s_{\rm NN}}$ = 5.02 TeV and Pb-Pb collisions at $\sqrt{s_{\rm NN}}$ = 2.76 TeV as a function of charged particle pair relative pseudorapidity, $\Delta\eta$, and azimuthal angle, $\Delta\varphi$, as well as collision centrality. The observable $\Delta p_{\rm T}\Delta p_{\rm T}$ features an explicit dependence on the transverse momentum of the produced particles. As such, it provides sensitivity to the correlation "hardness," i.e. how much high momentum transfer collisions contribute to the correlation dynamics. The measurements presented in this work will thus provide additional quantitative constraints on existing models.

2. Observable definition

Let ρ_1 and ρ_2 be one- and two-particle densities, respectively. The number correlation function is written in terms of the cumulant, i.e. $C_2 = \rho_2 - \rho_1\rho_1$, as: $R_2 = \frac{C_2}{\rho_1\rho_1}$. R_2 is by construction independent to first approximation of the detection efficiency, i.e. the detector efficiency cancels

PoS(ICPAQGP2015)032

out in the ratio. The transverse momentum correlation is defined as:

$$\langle \Delta p_t \Delta p_t \rangle(\eta_1, \varphi_1, \eta_2, \varphi_2) = \frac{\int \rho_2(\eta_1, \varphi_1, p_{t,1}, \eta_2, \varphi_2, p_{t,2}) \Delta p_{t,1} \Delta p_{t,2} dp_{t,1} dp_{t,2}}{\rho_2(\eta_1, \varphi_1, \eta_2, \varphi_2)} \tag{1}$$

The difference, $\Delta p_{t,i} = p_{t,i} - \langle p_{t,i} \rangle$, taken for each particle, measures deviations from the inclusive average momentum defined as

$$\langle p_{t,i} \rangle = \frac{\int \rho_1(\mathbf{p}_i) p_{t,i} dp_{t,i}}{\int \rho_1(\mathbf{p}_i) dp_{t,i}} \tag{2}$$

The observables in this analysis are discussed in detail in [5].

3. Data analysis

The data presented were acquired by the ALICE detector [6] in Pb-Pb collisions at $\sqrt{s_{\rm NN}} = 2.76$ TeV and p-Pb collisions at $\sqrt{s_{\rm NN}} = 5.02$ TeV in the years 2010 and 2013, respectively. For this analysis, the ALICE Inner Tracking System (ITS) and the Time Projection Chamber (TPC) are used to reconstruct charged particle tracks. The VZERO scintillator hodoscopes and the Silicon Pixel Detector (SPD) are used for the trigger definition. Track candidates in the TPC are selected in the pseudorapidity range $|\eta| < 1.0$. Track quality cuts in the TPC are based on the number of reconstructed space points (at least 70 out of a maximum of 159). Tracks are rejected from the final sample if their distance of closest approach to the reconstructed vertex in the longitudinal (d_Z) and radial (d_{xy}) directions are greater than 3.2 cm and 2.4 cm, respectively. Contamination from HBT effects in like-sign pairs is not removed in this measurement. An electron rejection cut is applied to suppress contribution from photon conversions. Four different charge pairs $(+-, -+, ++, --)$ are measured and the information is combined into a charge independent (CI) correlation function.

$$CI = \frac{1}{4}\{(+-) + (-+) + (++) + (--)\} \tag{3}$$

4. Results

Figures 1 and 2 display the correlation function R_2 and $\Delta p_{\rm T} \Delta p_{\rm T}$, respectively, in three different centrality classes in Pb-Pb collisions. Both correlation functions exhibit decreasing amplitude with increasing number of particles, which reflects correlation dilution with large multiplicity. While an away-side doubly peaked structure is observed in $\Delta p_{\rm T} \Delta p_{\rm T}$ correlation in the 0-5% centrality bin, there is no such feature for the R_2 correlation in the same centrality bin and it emerges only in more central (0-2%) collisions [7]. For the 30-40% centrality bin, the distributions are dominated by a large $\cos(2\Delta\varphi)$ modulation.

To characterize the various features observed in the correlation functions and to disantangle them, we proceed to fit the data with a Fourier decomposition in relative azimuth, $\Delta\varphi$, with coefficients that depend on $\Delta\eta$:

$$F(\Delta\eta, \Delta\varphi) = c_0(\Delta\eta) + 2 \times \sum_{n=1}^{6} c_n \cos(n\Delta\varphi). \tag{4}$$

The left and right panel of Figure 3 show the c_1 and c_2 coefficients, respectively, in selected centralities in Pb-Pb collisions at $\sqrt{s_{\rm NN}} = 2.76$ TeV. However, given the correlation functions have been symmetrized in $\Delta\eta$, we show the results only for $\Delta\eta > 0$. The first order coefficient, c_1, is influenced by the presence of the near-side peak in the correlation functions. One consequently observes positive values at all collision centralities for $\Delta\eta < 0.7$ and negative values otherwise.

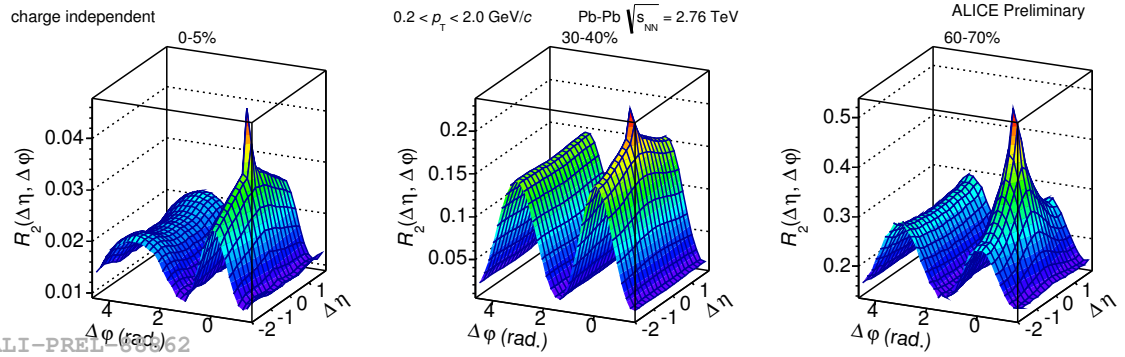

Figure 1. Correlation function R_2 for charge independent (CI) pairs ($0.2 < p_{\mathrm{T}} < 2.0$ GeV/c) in Pb-Pb collisions at $\sqrt{s_{\mathrm{NN}}} = 2.76$ TeV for selected collision centrality ranges.

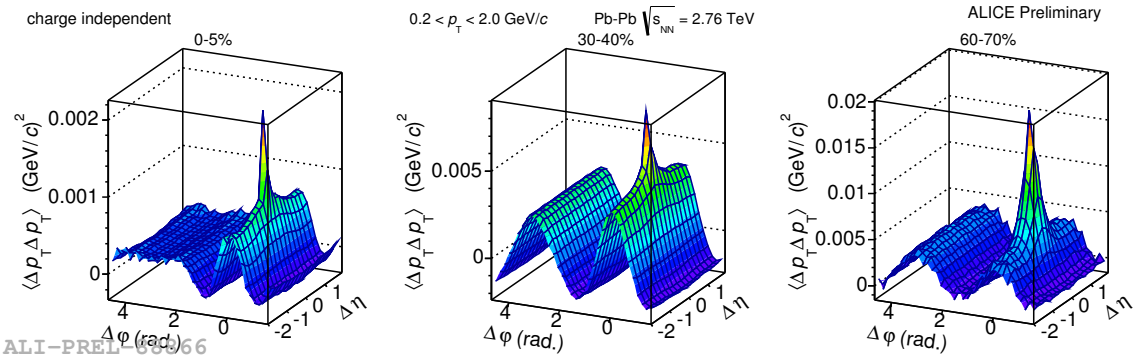

Figure 2. Correlation function $\Delta p_{\mathrm{T}} \Delta p_{\mathrm{T}}$ for charge independent (CI) pairs ($0.2 < p_{\mathrm{T}} < 2.0$ GeV/c) in Pb-Pb collisions at $\sqrt{s_{\mathrm{NN}}} = 2.76$ TeV for selected collision centrality ranges.

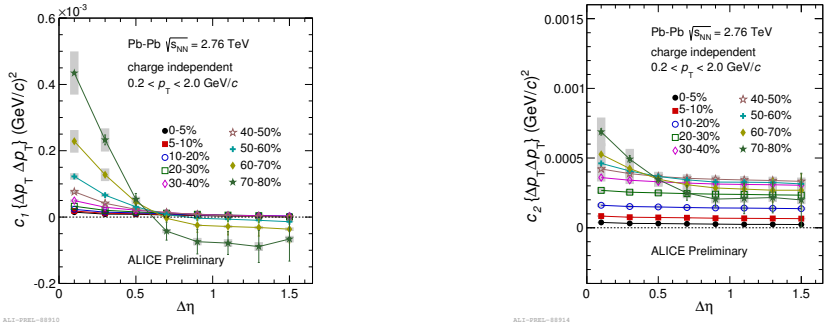

Figure 3. Harmonic coefficient $c_1\{\Delta p_{\mathrm{T}} \Delta p_{\mathrm{T}}\}$ (left) and $c_2\{\Delta p_{\mathrm{T}} \Delta p_{\mathrm{T}}\}$ (right) in Pb-Pb collisions at $\sqrt{s_{\mathrm{NN}}} = 2.76$ TeV.

Negative values reflect, in part, the fact that momentum conservation requires that particles should be emitted back-to-back in azimuth. The second order coefficient, c_2, depends on the collision centrality. We note that the values of c_2 exhibit a smaller dependence on $\Delta\eta$ for all results from centrality bins between 0 and 50% in Pb-Pb collisions.

While comparing the coefficients, $c_n\{R_2\}$ vs. $c_n\{\Delta p_{\mathrm{T}} \Delta p_{\mathrm{T}}\}$ in p-Pb collisions, we observe

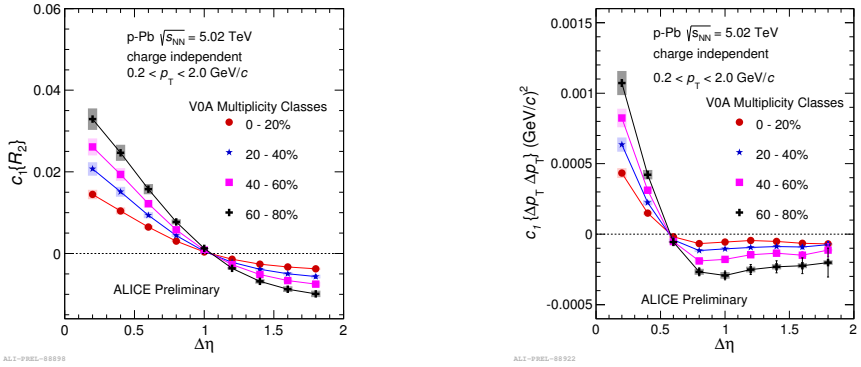

Figure 4. Harmonic coefficient $c_1\{R_2\}$ (left) and $c_1\{\Delta p_T \Delta p_T\}$ (right) in p-Pb collisions at $\sqrt{s_{NN}} = 5.02$ TeV.

different $\Delta\eta$ dependence for the correlation observables. As shown in Figure 4, $c_1\{\Delta p_T \Delta p_T\}$ changes sign earlier ($\Delta\eta \approx 0.6$) than $c_1\{R_2\}$ ($\Delta\eta \approx 1.2$). Figure 5 displays $c_2\{R_2\}$ (left panel) and $c_2\{\Delta p_T \Delta p_T\}$ (right panel). It is observed that $c_2\{\Delta p_T \Delta p_T\}$ saturates earlier in $\Delta\eta$ than $c_2\{R_2\}$.

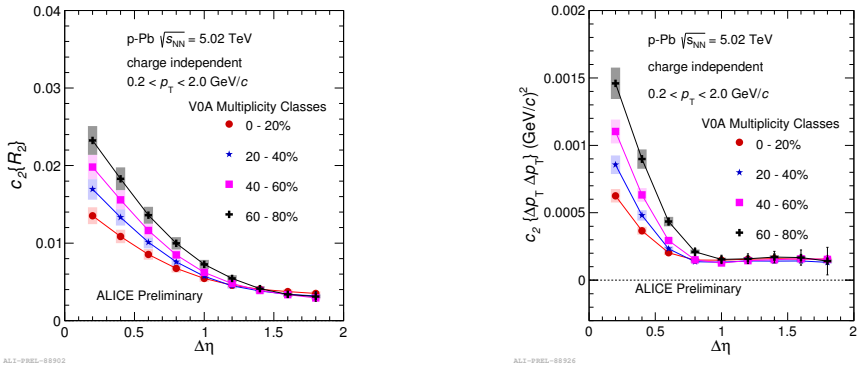

Figure 5. Harmonic coefficient $c_2\{R_2\}$ (left) and $c_2\{\Delta p_T \Delta p_T\}$ (right) in p-Pb collisions.

5. Summary

The first measurement of differential $\Delta p_T \Delta p_T$ correlations at the LHC energies are discussed in p-Pb and Pb-Pb collisions. $\Delta p_T \Delta p_T$ correlation shows an away-side doubly peaked structure in 0-5% centrality which in contrast to what is observed in R_2 correlation function in the same centrality in Pb-Pb collisions at $\sqrt{s_{NN}} = 2.76$ TeV. The harmonic coefficients obtained from $\Delta p_T \Delta p_T$ show a different evolution vs. $\Delta\eta$ as compared to those from R_2.

6. References

[1] J. Adams *et al.,* [STAR Collaboration], Phys. Rev. C **73** (2006) 064907.
[2] M. P. McCumber *et al.,* [PHENIX Collaboration], J. Phys. G **35** (2008) 104081.
[3] S. Chatrchyan *et al.,* [CMS Collaboration], Phys. Lett. B**724** (2013) 213.
[4] B. Abelev *et al.,* [ALICE Collaboration], Phys. Lett. B**719** (2013) 29.
[5] M. Sharma, C. A. Pruneau, Phys. Rev. **C79**, 024905 (2009)
[6] K. Aamodt *et al.,* [ALICE Collaboration], JINST, 3, (2008) S08002.
[7] B. Abelev *et al.,* [ALICE Collaboration], Phys. Lett. B**708** (2012) 249-264.